Synergistic Manipulation of Micro-Phosphorus and Sulphur Incorporation on Carbonaceous Cathode Endows Superior Zinc-Ion Storage Performance

Lai Yu[+], Jie Li[+], Nazir Ahmad, Xiaoyue He, Rong Liu, Xinyi Ma, Jianming Li, Anqiang Pan[*] and Genqiang Zhang[*]

Ms. J. Li, Mr. X. Y. He, Ms. R. Liu, Ms. X. Y. Ma, and Prof. G. Q. Zhang

Hefei National Laboratory for Physical Sciences at the Microscale, CAS Key Laboratory of Materials for Energy Conversion, Department of Materials Science and Engineering, University of Science and Technology of China, Hefei, Anhui 230026 China

Mr. L. Yu

New Energy Research Institute School of Environment and Energy South China University of Technology Higher Education Mega Center 382 East Waihuan Road, Guangzhou 510006, China

Prof. A. Q. Pan

School of Materials and Engineering, Xinjiang University, Urumqi, 830046, Xinjiang

Prof. J. M. Li

College of New Energy, Ningbo University of Technology, Ningbo, 315211, China

*To whom the correspondence should be referred. Email: pananqiang@xju.edu.cn; gqzhangmse@ustc.edu.cn.

[+] These authors contribute equally to this work.

1. Experimental section

1.1. Synthesis of PS-HPCNS

In a typical synthesis, 2 mmol 4,4'-thiodiphenol (4,4'-TDP), 1 mmol phytic acid (PA) and 16 mmol potassium hydroxide (KOH) were added into 15 mL the deionized water in order. They undergone an acid-base neutralization reaction to form potassium salts (denoted as TDP/PA-K) under stirring for 4 h. After dried at 90 ^{o}C, the TDP/PA-K salt was pyrolyzed at 800 ^{o}C for 2 h with a temperature increase rate of 2 °C min^{-1} in an argon atmosphere. The obtained product (denoted as C-TDP/PA-K) was further washed with 3 mol L^{-1} hydrochloric acid and deionized water, respectively, and dried overnight at 80 ^{o}C to obtain the final product of hierarchical porous carbon nanosheets with the incorporation of P and S (denoted as PS-HPCNS). The contrast sample of S doped porous carbon (denoted as S-PC) was obtained by only adding 2 mmol 4,4'-TDP and 4 mmol KOH while other conditions remained unchanged.

1.2. Characterizations

The field-emission scanning electron microscopy (FESEM, SU-8220) and transmission electron microscopy (Hitachi HT7700, JOEL, JEM-2010; Talos F200X) were used to investigated the morphologies of samples. The X-ray diffraction (XRD) patterns were collected on a Bruker D8 Advance X-Ray Diffractometer. The structures and surfaces were tested by Raman spectrometer (Renishaw inVia) with an excitation wavelength of 532 nm and Fourier transform infrared spectrometer (FTIR, Nicolet 8700). The chemical states of samples were analyzed by X-ray photoelectron spectroscopy (XPS, ESCALAB 250). Brunauer-Emmett-Teller (BET) specific surface area was measured by ASAP 2460 surface area system (Micromeritics).

1.3. Electrochemical measurements

The active materials were mixed with carbon black (Super-P) and

polytetrafluoroethylene preparation (PTFE) binder at a weight ratio of 8:1:1 in a mixed solution of ethanol and N-methyl-2 -pyrrolidinone (NMP). The slurries were pasted onto graphite paper and dried in a vacuum oven overnight at 100 °C. The an average mass loading was about ~1.4 mg cm^{-2}, and then they were assembled into LIR 2016 coin type cells in a glove box. The bare Zn foils were immersed in 0.5 M $InCl_3$ aqueous solutions for 10 minutes to form the Zn|In counter electrodes.[1] 2 M $ZnSO_4$ aqueous solution as the electrolyte, Whatman glass microfiber filters (GF/F) as the separator, and the voltage range was 0.01-1.9 V. The electrochemical test was performed on a Neware multichannel battery teste system. Cyclic voltammetry (CV) and electrochemical impedance spectroscopy (EIS) were investigated by using a Four-channel potentiostat CS3104 (Wuhan CorrTest Instruments Corp., Ltd.).

The following equations were used to calculate the energy density (E, Wh kg^{-1}) and power density (P, W kg^{-1}) of the ZHCs based on the mass of active material in cathode:[2]

$$E = I \int V dt / 3.6m \quad (1)$$

$$P = E/\Delta t \quad (2)$$

Where i is the current density, V is the voltage after ohmic drop, m represents the the mass of active material in cathode, and Δt is the discharge time.

1.4. Computational details

Density functional theory (DFT) calculations were carried out with the Vienna abinitio simulation package code[3, 4]. The generalized gradient approximation (GGA) in the form of the Perdew-Burke-Ernzerhof (PBE) functional were selected describe the exchange-correlation term[5]. A grid of 3 × 1 ×1 Monkhorst-Pack k-points was used for the structural relaxation. A vacuum layer of 25 Å is adopted in the in the z-directions to avoid the interaction between periodic layers. The energy cutoff was set to be 520 eV. The convergence criterion for the energy and maximum force for the optimization were set to 10^{-5} eV and 0.03

eV/Å, respectively. The adsorption energy is defined as:

$$E_{ads} = E_{Zn\text{-}surface} - E_{surface} - E_{Zn} \quad (3)$$

Where $E_{Zn\text{-}surface}$, E_{Zn} and $E_{surface}$ are the calculated total energies of the substrate with Zn atom, the clean substrate, and the isolated Zn atom, respectively.

2. Characterization

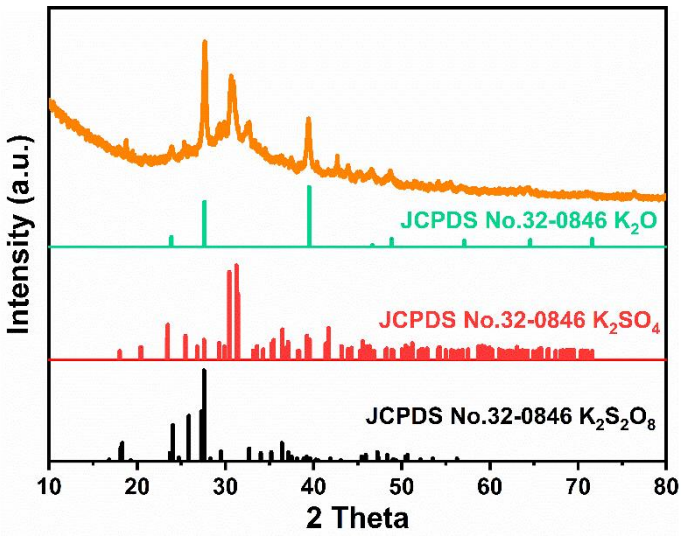

Fig. S1 The XRD pattern of C-TDP/PA-K.

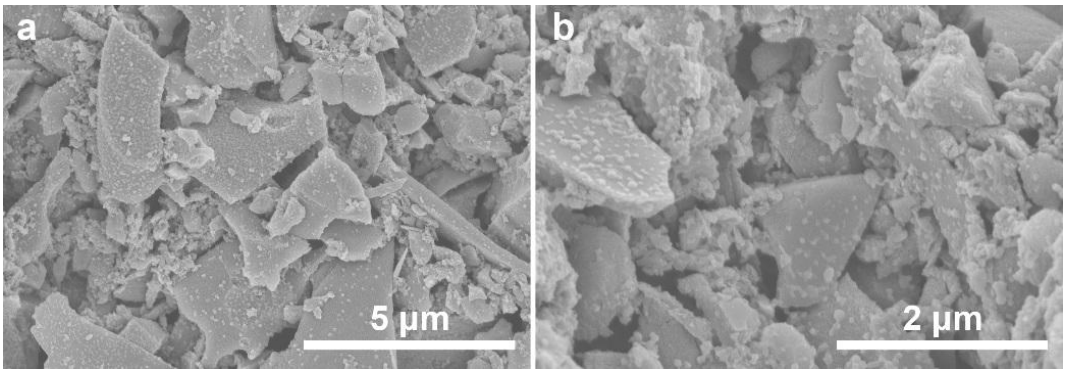

Fig. S2 The SEM images of S-PC.

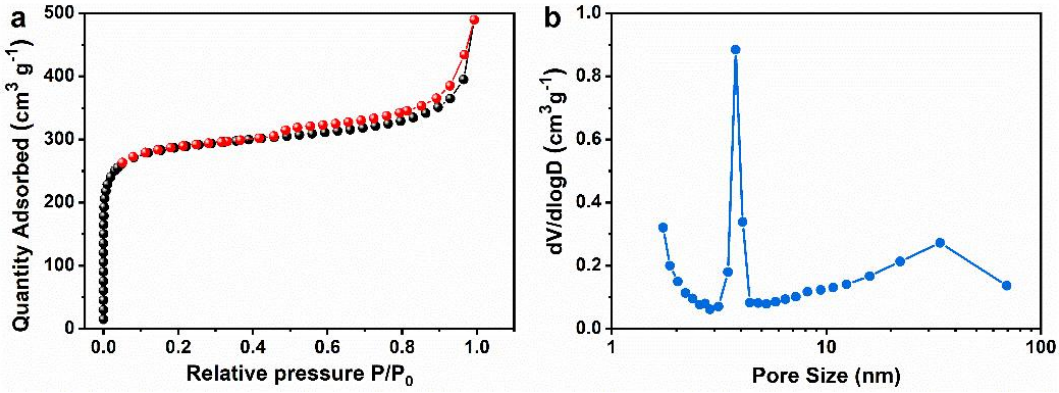

Fig. S3 (a) N_2 adsorption-desorption isotherms and (b) pore size distribution of S-PC materials.

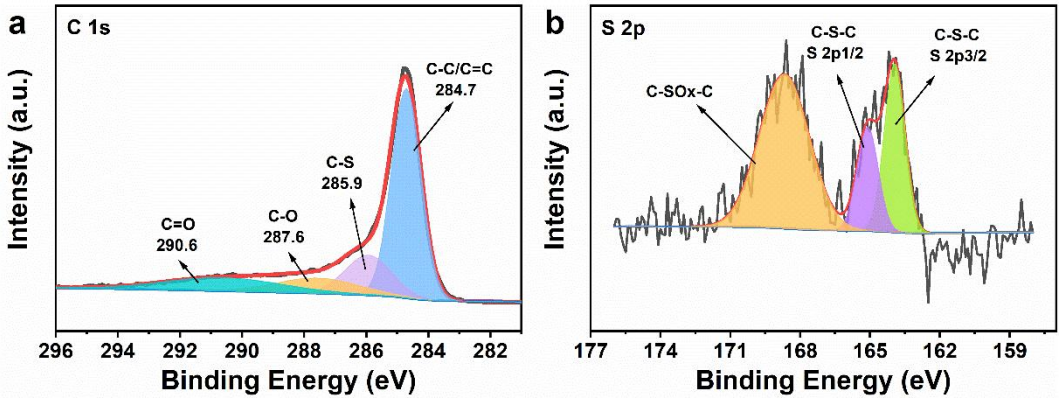

Fig. S4 (a) High-resolution C 1s spectra and (b) S 2p spectrum of S-PC.

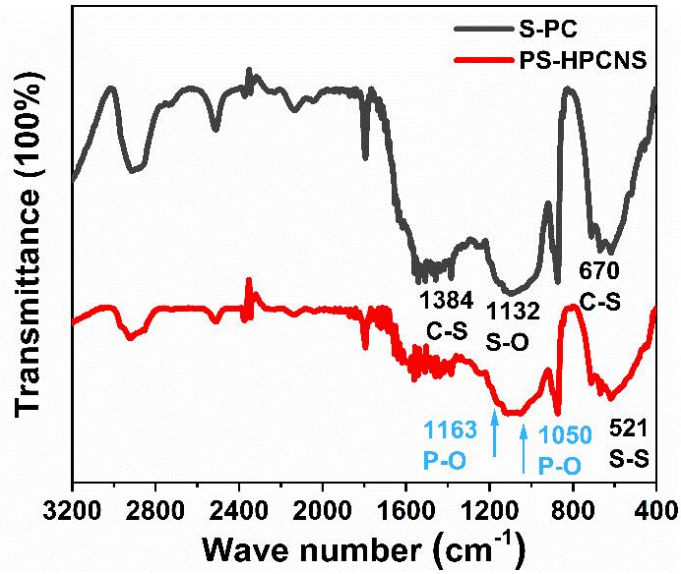

Fig. S5 FTIR spectra of S-PC and PS-HPCNS materials.

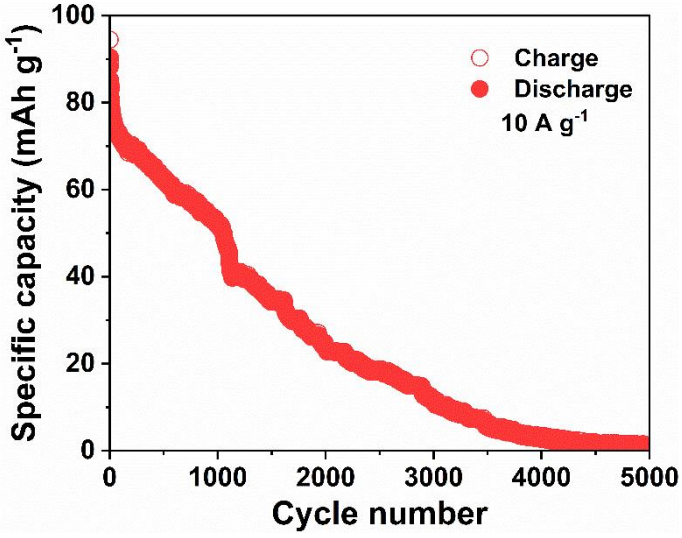

Fig. S6 Cycling performance of S-PC cathode at 10 A g^{-1}.

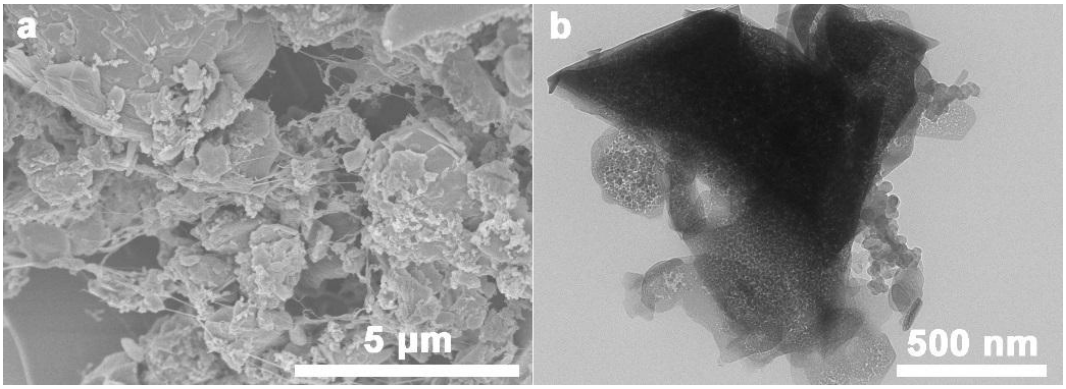

Fig. S7 (a) SEM and (b) TEM images of PS-HPCNS cathode after 10000 cycles at 10 A g^{-1}.

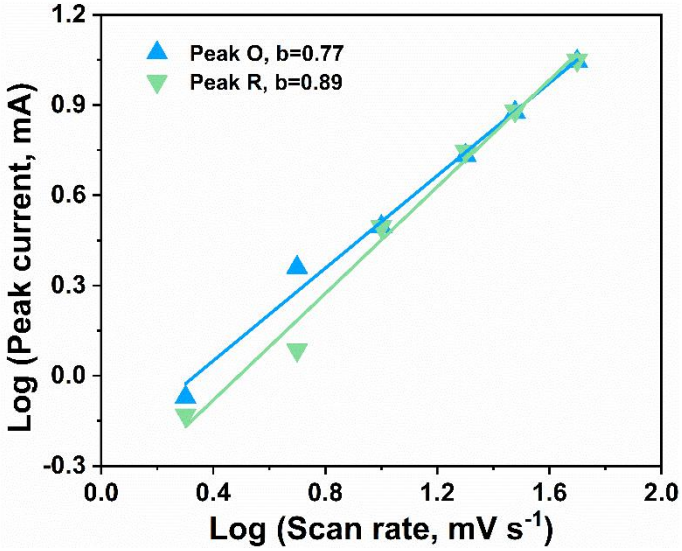

Fig. S8 The fitting plot between log(*i*) and log(*v*) of S-PC cathode.

.

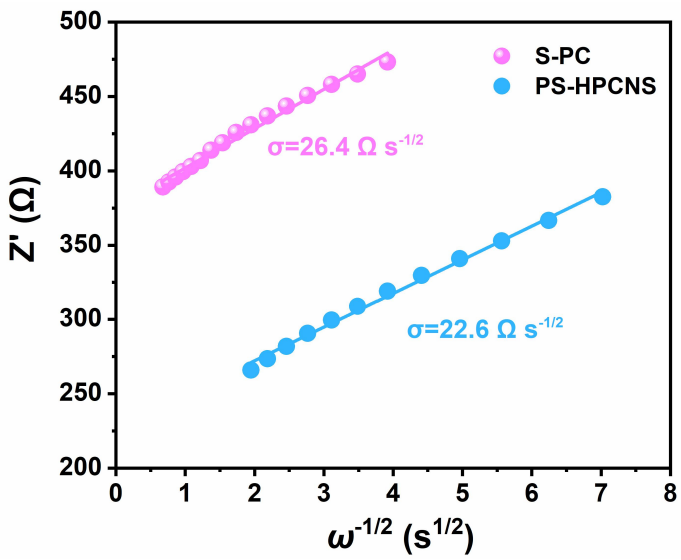

Fig. S9 Plots of *Z'* against $\omega^{-1/2}$ of the S-PC and PS-HPCNS cathodes based ZHCs.

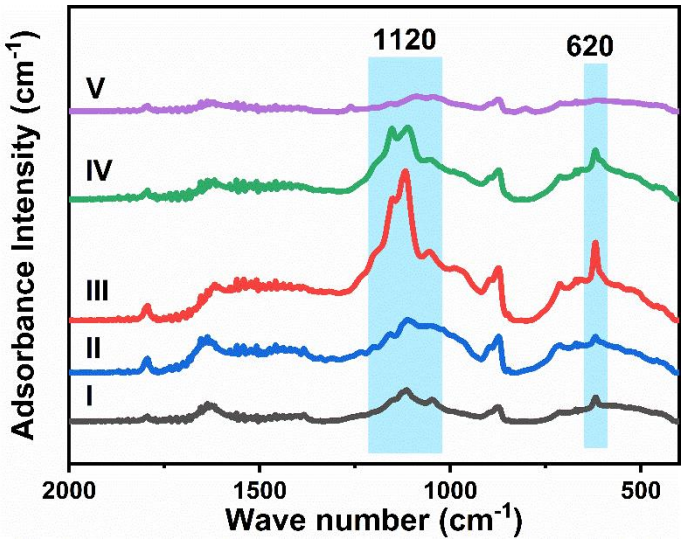

Fig. S10 Ex situ FTIR spectra of PS-HPCNS materials at different states.

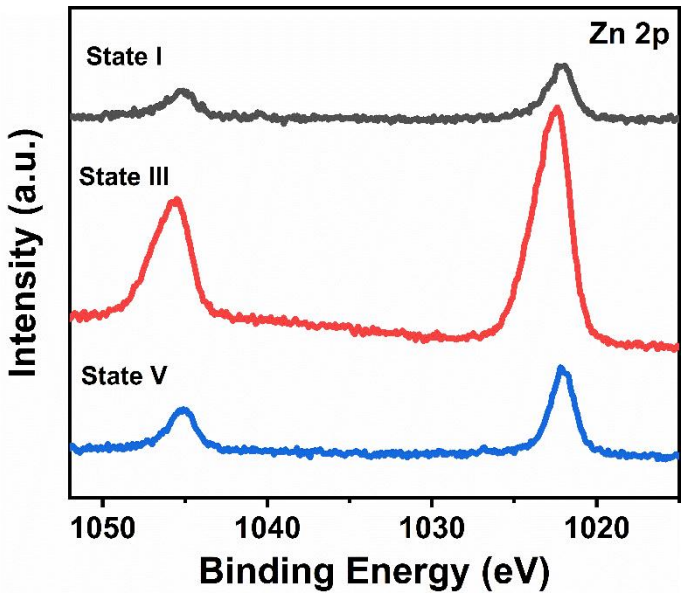

Fig. S11 Ex situ XPS spectra of Zn 2p for PS-HPCNS electrode at different states.

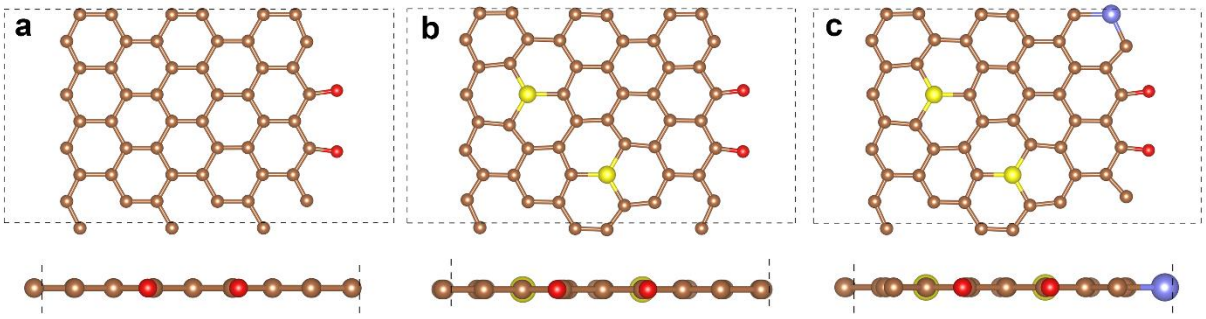

Fig. S12 The models of (a) pristine carbon, (b) S-PC and (c) PS-HPCNS. The brown, red, yellow and blue colors indicate C, O, S and P atom, respectively.

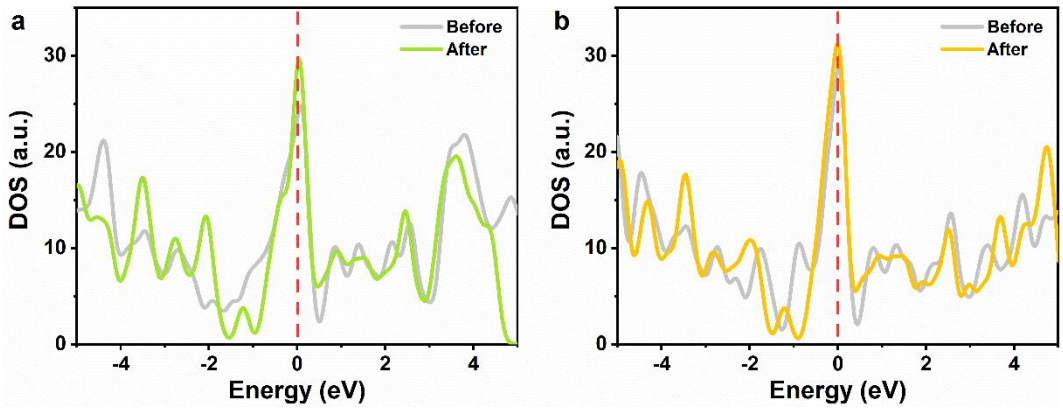

Fig. S13 DOS of (a) S-PC and (b) PS-HPCNS before/after Zn ions adsorption

Table S1. Electrochemical performance of aqueous ZHCs based on PS-HPCNS cathode compared with other reported carbon cathodes.

Materials	Voltage (V)	Capacity (mAh g^{-1})	Energy density (Wh kg^{-1})	Cycling stability	Ref.
PS-HPCNS	**0.01-1.9**	**240.1/0.2 A g^{-1}**	**139.3**	**84.6%/50000 cycles/10 A g^{-1}**	**This work**
LDC	0.2-1.8	127.7/0.5 A g^{-1}	97.6	–	[2]
AC	0.2-1.8	132/0.1 A g^{-1}	140.8	72%/20000 cycles/4 A g^{-1}	[6]
CNPK	0.2-1.8	103.2/0.1 A g^{-1}	81.1	101.8%/10000 cycles/5 A g^{-1}	[7]
OPC	0.2-1.8	132.7/0.2 A g^{-1}	82.36	87.6%/10000 cycles/1 A g^{-1}	[8]
ACNS	0.2-1.8	116.4/0.25 A g^{-1}	96.0	108.0%/10000 cycles/5 A g^{-1}	[9]
NPC	0-1.8	136.2/0.3 A g^{-1}	81.1	98.9%/60000 cycles/10 A g^{-1}	[10]
HPC-600	0.2-1.8	169.4/0.1 A g^{-1}	125.1	93.1%/60000 cycles/10 A g^{-1}	[11]
OPCNF	0.2-1.8	136.4/0.1 A g^{-1}	97.74	81%/50000 cycles/5 A g^{-1}	[12]
N, F, O-doped carbon	0.2-1.9	168.4/0.5 A g^{-1}	131.9	97.3%/9000 cycles/10 A g^{-1}	[13]
BCF	0.1-1.8	133.5/1 A g^{-1}	119.7	92%/20000 cycles/10 A g^{-1}	[14]

Reference

[1] D. Han, S. Wu, S. Zhang, Y. Deng, C. Cui, L. Zhang, Y. Long, H. Li, Y. Tao, Z. Weng, Q. H. Yang, F. Kang, Small **2020**, 16, 2001736.

[2] Y. Lu, Z. Li, Z. Bai, H. Mi, C. Ji, H. Pang, C. Yu, J. Qiu, Nano Energy **2019**, 66, 104132.

[3] J. G. F. Kresse, J., Phys. Rev. B **1996**, 54, 169.

[4] J. Hafner, J. Comput. Chem. **2008**, 29, 2044.

[5] K. B. John P. Perdew, * Matthias Ernzerhof, Phys. Rev. Lett **1996**, 77, 3865.

[6] Z. Wang, J. Huang, Z. Guo, X. Dong, Y. Liu, Y. Wang, Y. Xia, Joule **2019**, 3, 1289.

[7] H. Zhang, Z. Chen, Y. Zhang, Z. Ma, Y. Zhang, L. Bai, L. Sun, J. Mater. Chem. A **2021**, 9, 16565.

[8] Y. Zheng, W. Zhao, D. Jia, Y. Liu, L. Cui, D. Wei, R. Zheng, J. Liu, Chem. Eng. J. **2020**, 387, 124161.

[9] D. Wu, C. Ji, H. Mi, F. Guo, H. Cui, P. Qiu, N. Yang, Nanoscale **2021**, 13, 15869.

[10] X. Shi, H. Zhang, S. Zeng, J. Wang, X. Cao, X. Liu, X. Lu, ACS Materials Lett. **2021**, 3, 1291.

[11] L. Wang, M. Huang, J. Huang, X. Tang, L. Li, M. Peng, K. Zhang, T. Hu, K. Yuan, Y. Chen, J. Mater. Chem. A **2021**, 9, 15404.

[12] H. He, J. Lian, C. Chen, Q. Xiong, M. Zhang, Chem. Eng. J. **2021**, 421, 129786.

[13] L. Huang, Y. Xiang, M. Luo, Q. Zhang, H. Zhu, K. Shi, S. Zhu, Carbon **2021**, 185, 1.

[14] H. Fan, X. Hu, S. Zhang, Z. Xu, G. Gao, Y. Zheng, G. Hu, Q. Chen, T. S. AlGarni, R. Luque, Carbon **2021**, 180, 254.